


# The ‘double transition’: a novel electrocardiogram sign to discriminate posteroseptal accessory pathways ablated from the right endocardium from those requiring a left-sided or epicardial coronary venous approach

Patrizio Pascale <sup>1,2\*</sup>, Samuel Hunziker<sup>2</sup>, Arnaud Denis<sup>1</sup>, Jorge Rafael Gómez Flores<sup>3</sup>, Laurent Roten<sup>1</sup>, Ashok J. Shah<sup>1</sup>, Daniel Scherr<sup>1</sup>, Yuki Komatsu<sup>1</sup>, Khaled Ramoul<sup>1</sup>, Matthew Daly<sup>1</sup>, Mathieu LeBloa<sup>2</sup>, Etienne Pruvot<sup>2</sup>, Nicolas Derval<sup>1</sup>, Frédéric Sacher<sup>1</sup>, Mélèze Hocini<sup>1</sup>, Pierre Jaïs<sup>1</sup>, and Michel Haïssaguerre<sup>1</sup>

<sup>1</sup>Electrophysiology Department, Hôpital Cardiologique du Haut-Lévêque and Université de Bordeaux, IHU LIRYC ANR-10-IAHU-04, Bordeaux-Pessac, France; <sup>2</sup>Arrhythmia Unit, Cardiovascular Department, Centre Hospitalier Universitaire Vaudois and University of Lausanne, 1011 Lausanne, Switzerland; and <sup>3</sup>Electrophysiology Department, National Institute of Cardiology “Ignacio Chávez”, Mexico City, Mexico

Received 6 February 2020; editorial decision 18 June 2020; accepted after revision 19 June 2020

## Aims

The precise localization of manifest posteroseptal accessory pathways (APs) often poses diagnostic challenges considering that a small area may encompass AP that may be ablated from the right or left endocardium, or epicardially within the coronary sinus (CS). We sought to explore whether the QRS transition pattern in the precordial lead may help to discriminate the necessary ablation approach.

## Methods and results

Consecutive patients who underwent a successful ablation of a single manifest AP over a 5-year period were included. Standard 12-lead electrocardiograms were reviewed. A total of 273 patients were identified. Mean age was  $31 \pm 15$  years and 62% were male. Of the 110 identified posteroseptal AP, 64 were ablated from the right endocardium, 33 from the left endocardium, and 13 inside the CS. While a normal precordial QRS transition was most often observed, a subset of 33 patients presented an atypical ‘double transition’ pattern which specifically identified right endocardial AP. The combination of a q wave in V1 with a proportion of the positive QRS component in  $V1 < V2 > V3$ , predicted a right endocardial AP with a 100% specificity. In case of a positive QRS sum in V2, this ‘double transition’ pattern predicted a posteroseptal right endocardial AP with 99.5% specificity and 44% sensitivity. The positive predictive value was 97%. The only false positive was a midseptal AP. In the case of a negative or isoelectric QRS sum in V2, APs were located more laterally on the tricuspid annulus.

## Conclusion

The combination of a q wave in V1 with a double QRS transition pattern in the precordial leads is highly specific of a right endocardial AP and rules out the need for CS or left-sided mapping.

## Keywords

Wolff–Parkinson–White • Accessory pathway • Electrocardiogram • Delta wave • Precordial transition • Ablation

\* Corresponding author. Tel: +41 795565194; fax: +41 213140013. E-mail address: patrizio.pascale@chuv.ch

Published on behalf of the European Society of Cardiology. All rights reserved. © The Author(s) 2020. For permissions, please email: journals.permissions@oup.com.

## What's new?

- There are no identified electrocardiogram (ECG) signs that allows the specific identification of epicardial coronary venous accessory pathways (APs).
- The double QRS transition pattern in the precordial leads is a highly specific ECG finding which discriminates posteroseptal APs ablated from the right endocardium from those requiring a left-sided or epicardial coronary venous approach.
- In case of a double precordial transition in the precordial leads, the AP can be localized septally or laterally along the posterior tricuspid annulus depending on the polarity of the QRS in lead V2.

## Introduction

Radiofrequency catheter ablation has become the preferred treatment option for patients with symptomatic Wolff–Parkinson–White (WPW) syndrome. The success of the procedure depends on the accurate localization of the accessory pathway (AP) whose first step is provided by the analysis of the pre-excitation pattern on 12-lead electrocardiogram (ECG) during sinus rhythm. Several algorithms based on the delta wave and/or QRS polarity have been previously proposed to characterize the AP localization in WPW patients.<sup>1–10</sup> However, these criteria only provide an approximate indication of the AP localization and their accuracy is modest especially for certain locations.<sup>11</sup> More specifically, the precise localization of posteroseptal AP often poses a diagnostic challenge. This likely reflects the complex anatomy at the crux of the four cardiac chambers, where a small area may encompass AP that may be approached from the right or left endocardium, or require an ablation performed epicardially inside the coronary sinus (CS). Furthermore, the latter location has only been considered in a limited number of studies correlating the ECG patterns with the AP insertion site.<sup>1,6</sup>

Considering the differences in procedure risks and success rate depending on the need for a left-sided approach or a CS ablation,<sup>12–16</sup> an accurate anticipation of the precise location of posteroseptal AP is critical to inform the discussion and consent process with the patient and to guide the initial mapping strategy.

The purpose of the study was to identify novel ECG patterns that may help in the differential diagnosis of posteroseptal AP. More specifically, we sought to explore whether patterns of delta wave polarity or the QRS complex morphology in the precordial leads may help refine the localization of such AP.

## Methods

### Study population

The study population consisted of consecutive patients referred for ablation of manifest AP over a 5-year period. Patients with the following criteria were excluded: (i) presence of more than one anterogradely conducting AP, (ii) radiofrequency ablation aborted or unsuccessful, and (iii) Mahaim fibres.

A total of 273 patients were identified. Mean age was  $31 \pm 15$  years (range 9–76) and 62% were male. Written and informed consent was obtained from all patients.

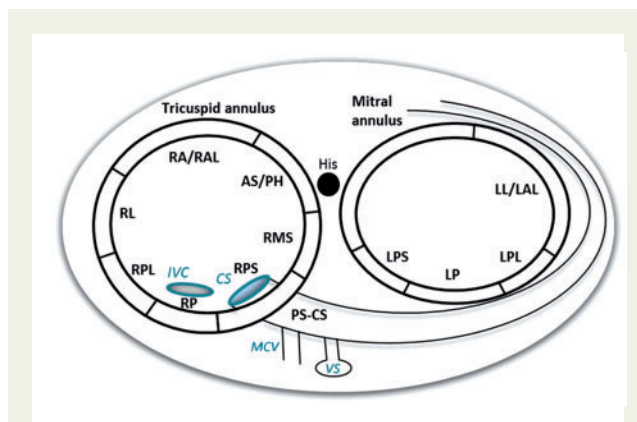


**Figure 1** Schematic representation of the atrioventricular annuli as viewed in the left anterior oblique view, with the classification of the accessory pathway locations. AS/PH, anteroseptal/parahissian; CS, coronary sinus; IVC, inferior vena cava; LL/LAL, left lateral/left anterolateral; LP, left posterior; LPL, left posterolateral; LPS, left endocardial posteroseptal; MCV, mid-cardiac vein; PS-CS, subepicardial posteroseptal; RA/RAL, right anterior/right anterolateral; RL, right lateral; RMS, right mid-septal; RP, right posterior; RPL, right posterolateral; RPS, right endocardial posteroseptal; VS, venous structure such as diverticula.

### Electrophysiological study

All procedures were performed in sinus rhythm after withdrawal of all antiarrhythmic drugs. Two diagnostic catheters were percutaneously inserted through the right femoral vein including a steerable quadri- or decapolar catheter positioned in the CS. Surface ECG and bipolar intracardiac electrograms (EGMs) were monitored continuously and stored on a computer-based digital amplifier/recorder system (Labsystem Pro, Boston Scientific, USA). Unipolar and bipolar EGM were band-pass filtered from 1 to 500 Hz and from 30 to 250 Hz, respectively.

### Mapping and ablation of accessory pathways

The ventricular insertion site of the AP were localized and ablated by mapping the earliest bipolar ventricular potential relative to the delta wave onset, associated with a QS pattern on the unipolar waveform, during sinus rhythm or atrial pacing as previously described.<sup>17</sup> Ablation energy source was most often standard radiofrequency. Irrigated radiofrequency was used when ablation was performed within the CS or for redo procedures. Left-sided AP were mapped using either a transseptal or retrograde aortic approach. A long sheath was used for right lateral and right anterior AP. Anterior, anteroseptal, and parahissian AP were targeted using either a left subclavian approach or a long sheath.

Regarding the mapping strategy of posteroseptal AP, CS ablation was not attempted prior to a meticulous left-sided mapping. Whenever favourable EGMs were recorded from the right posteroseptal (RPS) endocardial region, ablation was attempted from the tricuspid annular region adjacent to the CS ostium. Mapping outside and inside the CS was confirmed by fluoroscopy. Coronary sinus angiography was performed in case of suspected CS diverticulum or unsuccessful initial ablation attempts. If right-sided endocardial mapping appeared suboptimal, access to the left side was gained to map the posteroseptal region of the mitral annulus. The EGMs obtained from the left side were compared to those recorded from inside the CS. Ablation was attempted at the site with better EGMs but the right or left endocardium were preferentially targeted first.

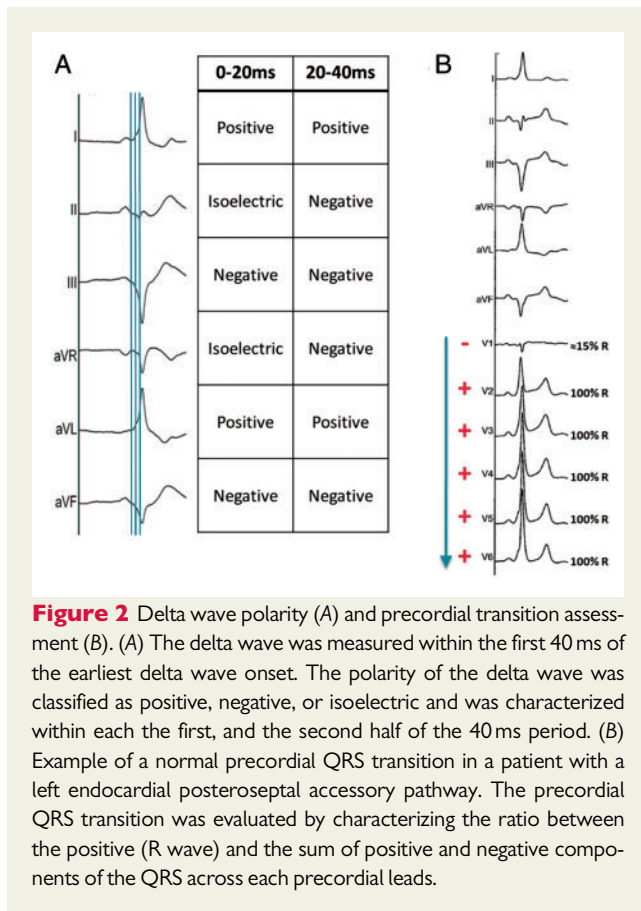


**Figure 2** Delta wave polarity (A) and precordial transition assessment (B). (A) The delta wave was measured within the first 40 ms of the earliest delta wave onset. The polarity of the delta wave was classified as positive, negative, or isoelectric and was characterized within each the first, and the second half of the 40 ms period. (B) Example of a normal precordial QRS transition in a patient with a left endocardial posteroseptal accessory pathway. The precordial QRS transition was evaluated by characterizing the ratio between the positive (R wave) and the sum of positive and negative components of the QRS across each precordial leads.

The successful ablation site was identified radiographically in the left anterior oblique view with the catheter recording the His-bundle potential pointing directly towards the operator. In this projection, the CS ostium was identified by a point located directly below on the same sagittal plane, on the shaft of the catheter placed within the CS.

### Classification of the accessory pathway location

AP locations were classified into three main regions further subdivided in 13 locations similar to the classification proposed by Arruda *et al.*<sup>1</sup> (Figure 1).

- (1) *Septal AP* were divided into five locations: (i) anteroseptal/parahissian from 1 o'clock to the area where a His-bundle potential was recorded; (ii) right mid-septal included AP located on the septal section of the tricuspid annulus comprised between the parahissian and the posteroseptal locations; (iii) RPS included AP located around the CS ostium; (iv) subepicardial posteroseptal (PS-CS) consisted of AP successfully ablated  $\geq 1$  cm within the CS including those ablated in the mid-cardiac vein, in diverticula or other venous structure; and (v) left posteroseptal (LPS) consisted of left endocardial AP ablated from 7 o'clock to 8 o'clock along the mitral annulus.
- (2) *Right free wall AP* were divided into four locations: (i) right anterior/right anterolateral from 1 o'clock to 10 o'clock; (ii) right lateral from 8 o'clock to 10 o'clock; (iii) right posterolateral from 7 o'clock to 8 o'clock; and (iv) right posterior from 5 o'clock to 7 o'clock.

- (3) *Left free wall AP* were divided into three locations: (i) left lateral/left anterolateral from 12 o'clock to 4 o'clock; (ii) left posterolateral from 4 o'clock to 5 o'clock; and (iii) left posterior from 5 o'clock to 7 o'clock.

### Electrocardiogram analysis

The standard resting 12-lead ECG was analysed at 25 mm/s sweep speed and with a standard gain of 1 mV/cm with a filter setting of 0.05 Hz (high pass) and 100 Hz (low pass). The 12 leads were recorded simultaneously. Two investigators blinded to the ablation results independently analysed the ECG. In case of disagreement, a consensus was obtained. The onset of the delta wave in each lead was measured from the onset of the earliest delta wave observed in any of the peripheral leads. The delta wave was measured within the first 40 ms of the earliest delta wave onset. The polarity of the delta wave was classified as positive, negative, or isoelectric and was characterized within each the first and the second half of the 40 ms period, as illustrated in Figure 2A.

The polarity and relative amplitude of each component of the QRS complexes were characterized in each lead. The precordial QRS transition was evaluated by characterizing the ratio between the positive (R wave) and the sum of positive and negative components of the QRS across each precordial leads (Figure 2B).

### Statistical analysis

Continuous variables are presented as arithmetic means  $\pm$  standard deviation. Categorical variables are expressed as absolute numbers and percentages. Categorical variables were compared with the  $\chi^2$  test or the Fisher's exact test, as appropriate. All tests were two-tailed, and statistical significance was assumed for  $P$ -values  $< 0.05$ . Statistical analysis was performed using the software SPSS, 17.0 (SPSS, Inc., Chicago, IL, USA).

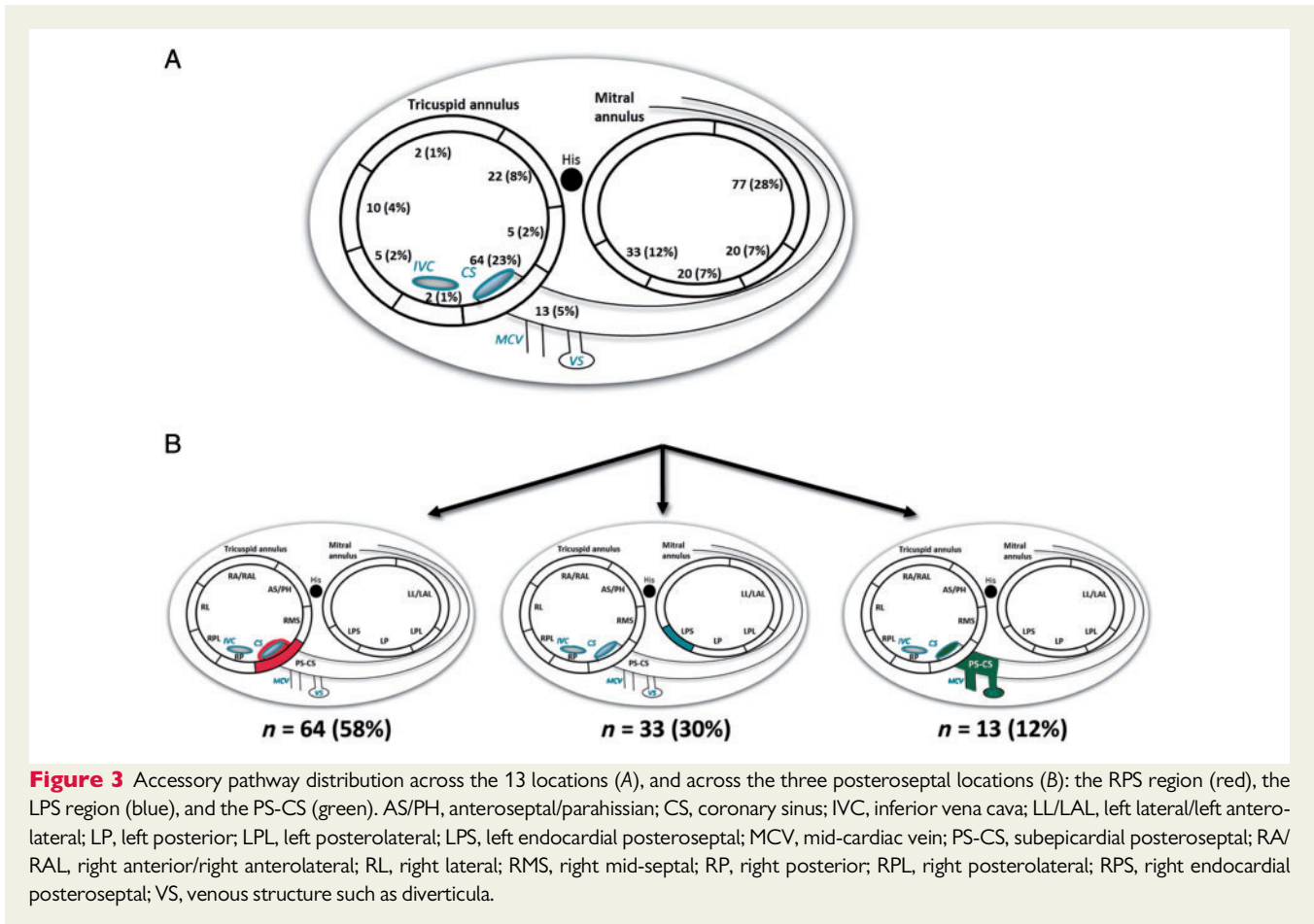
## Results

A total of 274 patients with a single manifest AP successfully ablated were identified. Two patients had Ebstein's anomaly. One previously published case was excluded from the analysis because of an atypical AP located at the collar of a right atrial appendage diverticulum.<sup>18</sup> The mean age was  $31 \pm 15$  years and 62% were male.

The distribution of the AP localizations is illustrated in Figure 3A. A total of 110 posteroseptal AP were identified, which represented 40% of the study population. Of these AP, 64 (58%) were ablated at the right endocardial posteroseptal region, 33 (30%) at the left endocardial posteroseptal region, and 13 (12%) inside the CS (Figure 3B).

### Delta wave polarity

The polarity of the delta wave in the inferior leads and V1 is reported in Table 1. No delta wave polarity pattern was found to specifically discriminate the different posteroseptal AP locations. A negative polarity of the initial 20 ms of the delta wave in lead II has been associated with AP ablated within the CS as reported by Arruda *et al.* This finding was indeed more often observed in PS-CS AP with 77% of cases displaying a negative delta wave compared to 41% and 39%, in RPS and LPS, respectively ( $P = 0.017$  and  $0.022$ , respectively). However, a negative initial delta wave in lead II was also often observed in right free wall (35%) and left posterior AP (40%). Of note, the same findings applied to patients with a negative initial delta wave in all inferior leads since all patients with a negative delta wave in lead



II, also displayed a negative delta wave in leads III and aVF. Using the stepwise diagnostic algorithm proposed by Arruda *et al.*,<sup>1</sup> a negative delta wave in lead II would provide a 77% sensitivity, 68% specificity and 18% positive predictive value (PPV) [95% confidence interval (CI) 9–30%] to identify a PS-CS AP.

Different combinations of inferior leads delta wave polarities were also evaluated. The combination of a positive initial delta wave (0–20 ms) in lead II, with negative delta waves in lead III and aVF, is expected to point towards a more right-sided location.<sup>5</sup> This pattern was only observed in nine patients (3%); eight with right endocardial AP (seven RPS, one right mid-septal), and one with a left-sided posteroseptal AP. Though the sensitivity was only 6%, this finding provided a 96% specificity and 89% PPV (95% CI 51–99%) to predict a right endocardial septal AP.

Similarly, we evaluated the combination of a negative or isoelectric initial delta wave (0–20 ms) in V1, combined with a negative delta wave in lead aVF to identify RPS AP as proposed by Arruda *et al.*<sup>1</sup> This combination provided a 58% sensitivity, 93% specificity, and 73% PPV to identify RPS AP (95% CI 58–84%). A higher specificity (96%) was found when the analysis included only a negative initial delta wave in both V1 and aVF, which provided a 45% sensitivity and 78% PPV (95% CI 61–90%). A positive delta wave in V1 provided limited specificity to predict a left-sided posteroseptal AP considering that

this feature was observed in most PS-CS AP (62%), and in a substantial number of RPS AP (14%).

### Precordial QRS transition

A normal precordial QRS transition with a progressively increasing R-wave proportion across the precordium was observed in most of the cases (Figure 2B). In a subset of patients, an atypical QRS transition pattern was observed with a proportion of the positive QRS component increasing from lead V1 to V2, and beyond V3, but decreasing between lead V2 and V3 (positive QRS component in V1 < V2 > V3). This pattern produced a ‘double transition’ as illustrated in Figure 4. The combination of a q wave in V1 with a proportion of the positive QRS component in V1 < V2 > V3 predicted a right endocardial AP with a 100% specificity (sensitivity 30%). This pattern was observed in 33 patients (12% of the study population). Of these patients, 28 patients had an RPS AP (including one at 5 o’clock), one had a right mid-septal AP, three had a right posterolateral AP, and one a right lateral AP. Of note, this double transition pattern was also specifically related to right endocardial AP when a q wave was lacking in V1 as long as the QRS was predominantly negative with a substantial degree of pre-excitation (defined as a QRS width > 130 ms). Including such cases, the double transition pattern yielded a 34% sensitivity and 100% specificity to identify right endocardial AP. Of the total

**Table 1** Polarity of the delta wave in the inferior leads and lead V1 for each AP localization

	Total (n = 273)	AS/PH (n = 22)	RSM (n = 5)	RPS (n = 64)	LPS (n = 33)	PS-CS (n = 13)	RA/RAL (n = 2)	RL (n = 10)	RPL (n = 5)	RP (n = 2)	LL/LAL (n = 77)	LPL (n = 20)	LP (n = 20)
<b>Lead II</b>													
Negative δ wave (0–20 ms)	64	0	0	26 (41%)	13 (39%)	10 (77%)	0	3 (30%)	2 (40%)	1 (50%)	0	1 (5%)	8 (40%)
Negative component of the δ wave (0–20 and/or 20–40 ms)	104	0	2 (40%)	41 (64%)	19 (58%)	12 (92%)	0	3 (30%)	4 (80%)	2 (100%)	3 (4%)	6 (30%)	12 (60%)
<b>Lead III</b>													
Negative δ wave (0–20 ms)	119	1 (5%)	3 (60%)	56 (88%)	19 (58%)	10 (77%)	0	7 (70%)	5 (100%)	1 (50%)	1 (1%)	5 (25%)	11 (55%)
Negative component of the δ wave (0–20 and/or 20–40 ms)	159	2 (9%)	4 (80%)	63 (98%)	31 (94%)	13 (100%)	0	8 (80%)	5 (100%)	2 (100%)	2 (3%)	11 (55%)	18 (90%)
<b>Lead aVF</b>													
Negative δ wave (0–20 ms)	96	0	2 (40%)	46 (72%)	16 (48%)	10 (77%)	0	6 (60%)	3 (60%)	1 (50%)	1 (1%)	2 (10%)	9 (45%)
Negative component of the δ wave (0–20 and/or 20–40 ms)	143	1 (5%)	3 (60%)	59 (92%)	30 (91%)	12 (92%)	0	6 (60%)	5 (100%)	2 (100%)	1 (1%)	8 (40%)	16 (80%)
<b>Lead V1</b>													
Negative δ wave (0–20 ms)	70	6 (27%)	5 (100%)	45 (70%)	3 (9%)	3 (23%)	0	3 (30%)	3 (30%)	1 (50%)	0	0	1 (5%)
Negative component of the δ wave (0–20 and/or 20–40 ms)	106	17 (77%)	5 (100%)	54 (84%)	6 (18%)	3 (23%)	1 (50%)	9 (30%)	4 (40%)	2 (100%)	3 (4%)	1 (5%)	1 (5%)
Positive δ wave (0–20 ms)	150	16 (73%)	0	9 (14%)	20 (61%)	8 (62%)	2 (100%)	7 (70%)	2 (40%)	1 (50%)	57 (74%)	15 (75%)	13 (65%)
Positive component of the δ wave (0–20 and/or 20–40 ms)	190	16 (73%)	0	14 (22%)	24 (73%)	11 (85%)	2 (100%)	9 (90%)	2 (40%)	1 (50%)	73 (95%)	19 (95%)	19 (95%)

AP, accessory pathway; AS/PH, anterosseptal/parahissian; LL/LAL, left lateral/left anterolateral; LP, left posterior; LPL, left posterolateral; LPS, left endocardial posteroseptal; PS-CS, subcardiac posteroseptal; RMS, right mid-septal; RPS, right endocardial posteroseptal; RA/RAL, right anterior/right anterolateral; RL, right lateral; RP, right posterior; RPL, right posterolateral.

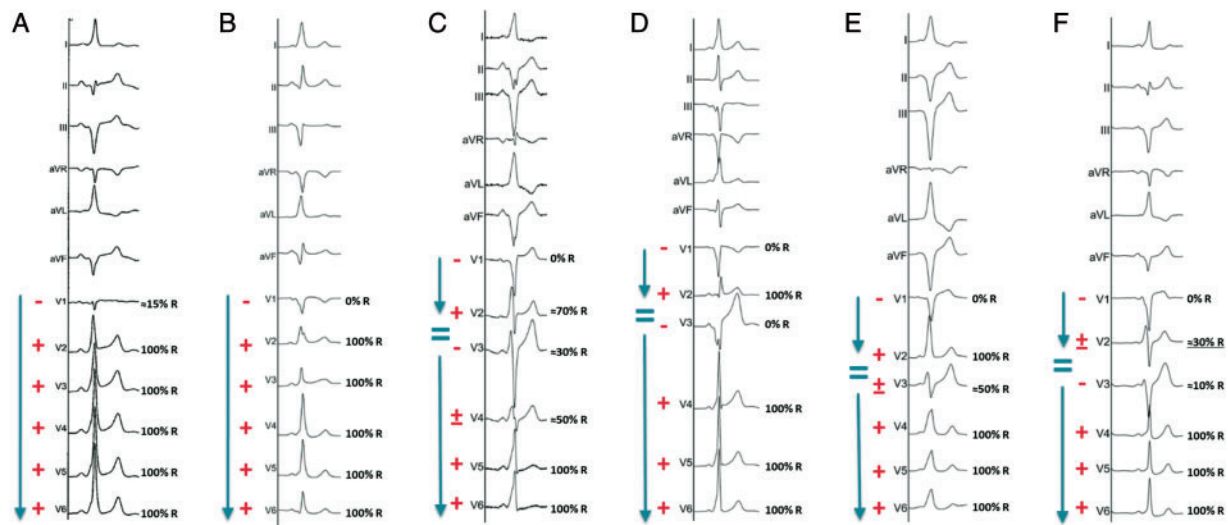


**Figure 4** Representative examples of 12-lead electrocardiograms. In left endocardial (A) and subepicardial (B) posteroseptal accessory pathways, a normal precordial lead transition was observed (blue arrow) with a progressively increasing R-wave proportion (displayed in percent) across the precordium. On the other hand, an abnormal transition pattern was specifically observed in a subset of patients with right endocardial accessory pathways (C–F): a ‘double precordial transition’ is observed (blue arrows), with a proportion of the positive QRS component in  $V1 < V2 > V3$ . The QRS polarity in lead V2 allowed to further localize the accessory pathway along the tricuspid annulus: a positive QRS sum indicated a posteroseptal right endocardial accessory pathway (C–E), whereas a negative or isoelectric QRS sum in lead V2 predicted a more lateral localization as illustrated in a posterolateral right accessory pathway (F).

population, this pattern helped to identify almost about one out of seven AP ( $n = 37$ ).

Additionally, a more precise localization of the AP could be achieved by assessing the QRS polarity sum in V2. Namely, in case of a positive QRS sum in V2 (Figure 4A–C), this ‘double transition’ pattern could identify an RPS AP with a specificity of 99.5%, a sensitivity of 44%, and a PPV of 97% (95% CI 80–100%). The only false positive was a right mid-septal AP. On the other hand, in case of a negative or equiphasic QRS sum in V2 (Figure 4D), the AP was localized more laterally with respect to the middle of the cavotricuspid isthmus. This pattern provided 99.6% specificity, 27% sensitivity, and 80% PPV (95% CI 30–99%) to identify a right posterolateral or lateral AP. The only false positive was an RPS AP in a patient with Ebstein’s anomaly and complete right bundle branch block after ablation.

A proposed algorithm based on the ‘double transition’ pattern is illustrated in Figure 5.

## Discussion

### Main findings

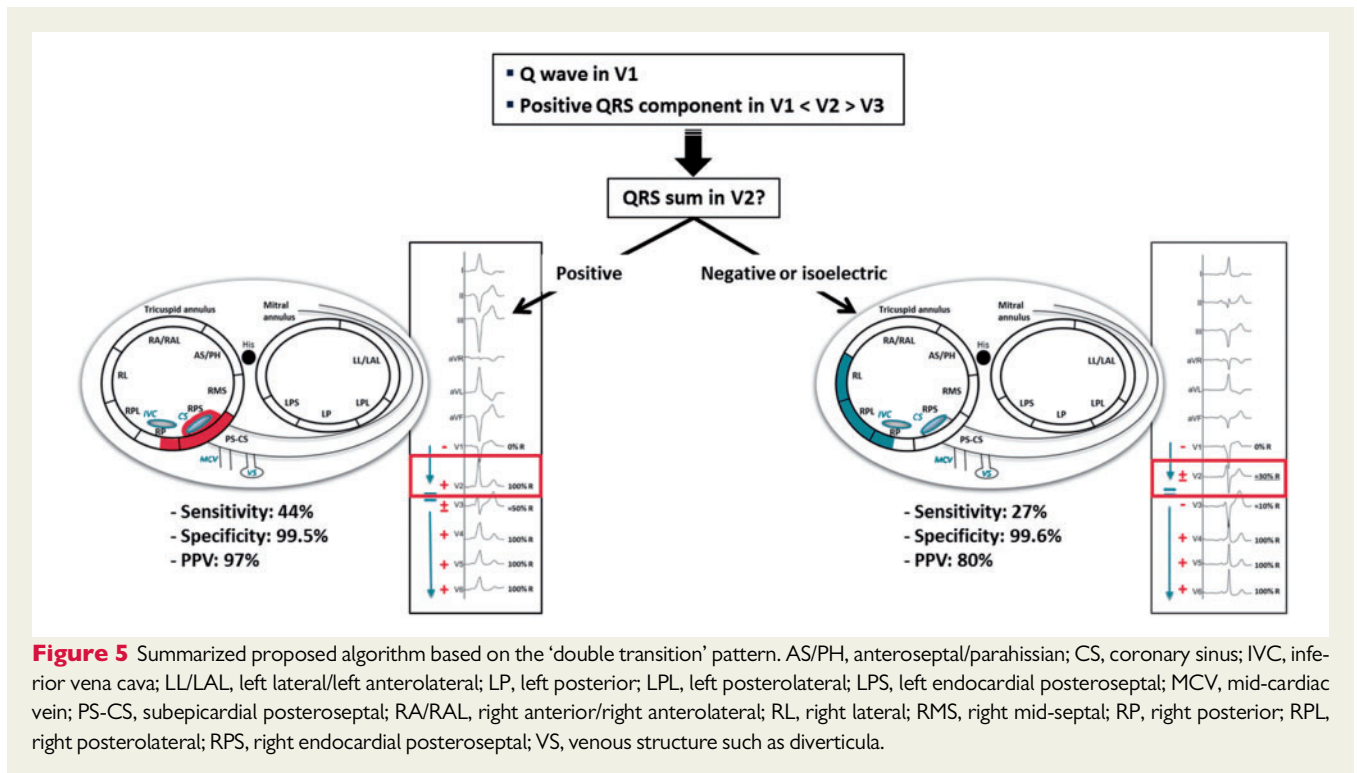
The major finding of our study is the identification of a novel ECG sign which allows to specifically discriminate posterior and posteroseptal AP that are successfully ablated from the right endocardium. The ECG sign consisted in the association of either a q wave or a predominantly negative wide QRS in V1, with a proportion of the positive precordial QRS component in  $V1 < V2 > V3$ , producing a ‘double precordial transition’ pattern. Out of a study population of 273 patients, this pattern was 100% specific of an AP that could be

ablated from the right endocardium and allowed to rule out the need for a left-sided approach or an ablation performed within the CS. Moreover, our study showed that the AP localization could be further refined depending on the QRS polarity in V2. Namely, in case of a positive QRS, the AP was localized on the right endocardial posteroseptal region, whereas in case of a negative or isoelectric in V2, the AP was localized more laterally on the tricuspid annulus.

This double transition pattern may help to characterize the AP localization of almost about one out of seven AP referred for ablation.

### Subepicardial accessory pathway: previous studies

Our data adds to a number of previously published studies based on the analysis of the delta wave and/or the QRS polarity.<sup>1–8</sup> Regarding the specific characterization of posteroseptal AP, the goal of most algorithms was to discriminate the laterality between right or left endocardial localizations. To our knowledge, only a limited number of studies have included in their analysis epicardially situated AP requiring ablation performed within the CS.<sup>1,6,16,19</sup> Arruda et al. developed a stepwise ECG algorithm based on the analysis of the polarity of the delta wave within the initial 20 ms of the pre-excitation. In the absence of a suspected left free wall AP, which was based on the polarity of the delta wave in lead I and V1, the identification of a negative delta wave in lead II was specifically associated with subepicardial AP ablated within the CS (100% sensitivity and specificity). In the present study, we found that a negative delta wave was indeed significantly more often observed in PS-CS AP compared to RPS and LPS AP. However, the specificity and sensitivity of that finding were low considering that about 40% of endocardial posteroseptal (left and right),



left posterior and right free wall AP, all displayed a negative delta wave in lead II. Accordingly, its sensitivity, specificity, and PPV in predicting a subepicardial AP were 77%, 68%, and 18%, respectively. Interestingly, our findings compare to the 70% sensitivity reported in a latter study by Arruda's group on a much larger number of subepicardial AP ( $n = 126$ ).<sup>16</sup>

The finding of a negative delta wave in all inferior leads has been regarded by some authors as suggestive of an RPS AP, generally related to the CS orifice region.<sup>5</sup> In our study population, this finding provided the exact same information as a negative delta wave in lead II with respect to the AP localization, since all of these patients also displayed a negative initial delta wave in lead III and aVF. Accordingly, this combination rather suggested a subepicardial AP localization though with limited specificity.

Takahashi *et al.*<sup>6</sup> evaluated the initial 40 ms of the delta wave in order to identify AP ablated within the CS from a selected population of 117 patients with manifest posteroseptal AP. They found that a negative delta wave in lead II was more often observed in AP ablated within the CS compared to those ablated right or left endocardially (87% vs. 21%,  $P < 0.01$ ). The sensitivity of this finding was quite high in this selected population of posteroseptal AP (87%), but the specificity and PPV were lower (79% and 50%, respectively). They also observed that a positive delta wave in lead aVR was more often observed in subepicardial AP compared to RPS and LPS AP (57% vs. 9%,  $P < 0.01$ ). The sensitivity, specificity, and PPV of this finding were 52%, 91%, and 62%. Moreover, among posteroseptal AP, a negative delta wave in V1 was present only in right endocardial posteroseptal AP (28% vs. 0%,  $P < 0.01$ ). Considering the different characterization of the delta wave polarity in our study, these results cannot be directly

compared. Notwithstanding, a positive delta wave in lead aVR, in both the first and second half of the 40 ms period, was specific of AP localized in the posteroseptal region but was rarely observed in our study population. This finding was observed in only 15% of PS-CS AP compared to 3% and 6% in RPS and LPS AP, respectively ( $P = 0.07$  and 0.31, respectively). Regarding the negative delta wave polarity in V1 as defined in their study, this finding was indeed specific of right endocardial AP in our study population. However, a negative delta wave was also observed in LPS and PS-CS AP, with a prevalence of 12% and 15%, respectively (as compared to 69% in RPS AP,  $P < 0.01$  for both comparisons).

Based on the data discussed here and on our study results, no evidence seem to support that a specific ECG pattern allows to selectively identify subepicardial AP on standard sinus rhythm ECG. Conceptually, the identification of such a pattern seems unlikely considering the proximity and overlap of structures in that region. It seems rather more realistic to aim for the identification of criteria that are specific for AP located at some distance of the overlapped endo- and epicardial components of the septum and the left atrium, as done in the present study.

### Delta wave polarity combinations

Different combinations of delta wave polarity in V1 and in the inferior leads were evaluated in order to accurately localize AP in the posteroseptal region. In the stepwise algorithm proposed by Arruda *et al.*, left free wall AP were first identified based either on the polarity of the initial delta wave (0–20 ms) in lead I (isoelectric or negative), or a R wave  $\geq$  S wave in V1. As a second step, subepicardial AP were

identified based on the delta wave polarity in lead II as previously discussed. RPS AP were identified based on the combination of a negative, or isoelectric, initial delta wave in V1, combined with a negative delta wave in lead aVF. In our study population, this pattern was fairly specific and provided 58% sensitivity, 93% specificity, and 73% PPV. Its specificity could be further increased when only negative delta waves were considered in both V1 and aVF (45% sensitivity, 96% specificity, and 78% PPV). Though somewhat more sensitive, this pattern remained however less specific than the 'double transition' pattern.

The delta wave polarity comparison between lead II and lead III has been proposed to discriminate AP more likely to be approachable from the right side: the larger the negative delta wave in lead III relative to lead II,<sup>19</sup> the more likely a posteroseptal AP will be ablated on the right endocardial side. Similarly, a positive initial delta wave (0–20 ms) in lead II combined with a negative delta wave in lead III and aVF has been shown to point towards an RPS AP.<sup>5</sup> The latter pattern was rarely observed in our study population ( $n = 9$ ) but was indeed fairly specific of a right endocardial AP (mostly RPS) with only one LPS. The sensitivity of this finding was only 6% but it provided a 96% specificity and 89% PPV.

## The double transition and QRS polarity in V2

The ECG pattern consisting of a 'double precordial transition' was specifically associated with right endocardial posterior and posteroseptal AP. While this association has not been specifically reported so far, Xie et al.<sup>8</sup> noticed in their study evaluating the polarity and morphology of the QRS that, among patients with RPS AP, 5 out of 11 of them (45%) had 'a higher R wave in leads V2 and V4 than in V3'. Interestingly, this proportion is similar as the one observed in our study population (i.e. 44%).

The mechanism underlying this pattern remains uncertain. Lead V2 and V3 face the right free wall and, rearward, the septum. Consistent with this, both leads have been shown to be useful for the identification of right septal or right free wall AP. In case of a 'double precordial transition', we found that the lead polarity in V2 was useful to localize the AP along the posterior tricuspid annulus. Namely, a positive QRS identified AP localized septally, whereas a negative or isoelectric QRS in lead V2, identified AP localized laterally with respect to the middle of the cavotricuspid isthmus. Similar to our findings, D'Avila et al.<sup>7</sup> found that among right-sided AP with a predominantly negative QRS complex in lead III, all 11 right lateral AP showed a negative QRS complex in V2, whereas most RPS AP displayed a positive QRS. Likewise, Fitzpatrick et al.<sup>4</sup> found that the most significant variable to discriminate right free wall from right septal AP was the precordial transition: a precordial transition at or before lead V3 (i.e. either a dominant R wave or equiphasic R/S wave in lead V3) indicated a septal location, whereas a QRS transition at or after lead V4, indicated a lateral location.

The relative negativity of the QRS in lead V3 with respect to lead V2, as seen with the 'double transition', does not seem to be specifically attributable to the fused septal activation resulting from conduction over the atrioventricular node and the AP. Indeed, while some degree of fusion cannot be excluded, this pattern was also observed during maximal pre-excitation in over 80% of our study population and, more importantly, it has also been observed for ventricular

arrhythmias originating from the posterolateral tricuspid annulus,<sup>20</sup> or near the crux of the heart, which are expected to reproduce maximally pre-excited posteroseptal AP.<sup>21</sup>

## Clinical implications

This novel ECG pattern allows the accurate anticipation of the localization about one out of seven AP addressed for ablation. Therefore, it provides important information in terms of procedure planning and to guide the initial mapping strategy. Importantly, considering that it provides a 100% specificity to identify AP accessible via a right-sided approach outside of the CS, knowledge of this pattern may be critical to inform the discussion and consent process with the patient, considering differences in risks and expected success rate depending on the need for a left-sided approach or a CS ablation. These considerations are all the more relevant for patients with asymptomatic pre-excitation considering that the role of ablation in this situation is less clear.

## Study limitations

One limitation of the study is the fact that the AP localization was based on the last radiofrequency application site which allowed the durable elimination of the AP. Some of these AP, especially those from the posteroseptal area, may actually overlap/extend in adjacent areas and require ablation on contiguous sites such as applications on both endocardial sides, or on the left endocardium combined with CS applications. This limitation is however inherent to all similar studies. Another limitation regarding posteroseptal pathways pertains to our ablation strategy. In order to limit risks to the patient, radiofrequency application within the CS was not performed before ruling out a possibly successful ablation from the left endocardial side. This strategy may possibly underrepresent the prevalence of subepicardial AP compared to an ablation strategy performing CS ablation more liberally.

## Conclusions

A double QRS transition pattern in the precordial leads is a specific finding which discriminates posterior and posteroseptal AP that can be successfully ablated from the right endocardium without the need for epicardial coronary venous or left-sided mapping.

**Conflict of interest:** none declared.

## Data availability

The data underlying this article will be shared on reasonable request to the corresponding author.

## References

1. Arruda MS, McClelland JH, Wang X, Beckman KJ, Widman LE, Gonzalez MD et al. Development and validation of an ECG algorithm for identifying accessory pathway ablation site in Wolff-Parkinson-White syndrome. *J Cardiovasc Electrophysiol* 1998;**9**:2–12.
2. Boersma L, Garcia-Moran E, Mont L, Brugada J. Accessory pathway localization by QRS polarity in children with Wolff-Parkinson-White syndrome. *J Cardiovasc Electrophysiol* 2002;**13**:1222–6.
3. Chiang CE, Chen SA, Teo WS, Tsai DS, Wu TJ, Cheng CC et al. An accurate stepwise electrocardiographic algorithm for localization of accessory pathways in patients with Wolff-Parkinson-White syndrome from a comprehensive analysis of delta waves and R/S ratio during sinus rhythm. *Am J Cardiol* 1995;**76**:40–6.



4. Fitzpatrick AP, Gonzales RP, Lesh MD, Odin GW, Lee RJ, Scheinman MM. New algorithm for the localization of accessory atrioventricular connections using a baseline electrocardiogram. *J Am Coll Cardiol* 1994;**23**:107–16.
5. Fox DJ, Klein GJ, Skanes AC, Gula LJ, Yee R, Krahn AD. How to identify the location of an accessory pathway by the 12-lead ECG. *Heart Rhythm* 2008;**5**:1763–6.
6. Takahashi A, Shah DC, Jais P, Hocini M, Clementy J, Haissaguerre M. Specific electrocardiographic features of manifest coronary vein posteroseptal accessory pathways. *J Cardiovasc Electrophysiol* 1998;**9**:1015–25.
7. d'Avila A, Brugada J, Skeberis V, Andries E, Sosa E, Brugada P. A fast and reliable algorithm to localize accessory pathways based on the polarity of the QRS complex on the surface ECG during sinus rhythm. *Pacing Clin Electrophysiol* 1995;**18**:1615–27.
8. Xie B, Heald SC, Bashir Y, Katritsis D, Murgatroyd FD, Camm AJ *et al*. Localization of accessory pathways from the 12-lead electrocardiogram using a new algorithm. *Am J Cardiol* 1994;**74**:161–5.
9. Iturralde P, Araya-Gomez V, Colin L, Kershenovich S, de Micheli A, Gonzalez-Hermosillo JA. A new ECG algorithm for the localization of accessory pathways using only the polarity of the QRS complex. *J Electrocardiol* 1996;**29**:289–99.
10. Haghjoo M, Mahmoodi E, Fazelifar AF, Alizadeh A, Hashemi MJ, Emkanjoo Z *et al*. Electrocardiographic and electrophysiologic predictors of successful ablation site in patients with manifest posteroseptal accessory pathway. *Pacing Clin Electrophysiol* 2007;**31**:103–11.
11. Katsouras CS, Grekas GF, Goudevenos JA, Michalis LK, Kolettis T, Economides C *et al*. Localization of accessory pathways by the electrocardiogram: which is the degree of accordance of three algorithms in use? *Pacing Clin Electrophysiol* 2004;**27**:189–93.
12. Belhassen B, Rogowski O, Glick A, Viskin S, Ilan M, Rosso R *et al*. Radiofrequency ablation of accessory pathways: a 14 year experience at the Tel Aviv Medical Center in 508 patients. *Isr Med Assoc J* 2007;**9**:265–70.
13. Sacher F, Wright M, Tedrow UB, O'Neill MD, Jais P, Hocini M *et al*. Wolff-Parkinson-White ablation after a prior failure: a 7-year multicentre experience. *Europace* 2010;**12**:835–41.
14. Solomon AJ, Tracy CM, Swartz JF, Reagan KM, Karasik PE, Fletcher RD. Effect on coronary artery anatomy of radiofrequency catheter ablation of atrial insertion sites of accessory pathways. *J Am Coll Cardiol* 1993;**21**:1440–4.
15. Stavrakis S, Jackman WM, Nakagawa H, Sun Y, Xu Q, Beckman KJ *et al*. Risk of coronary artery injury with radiofrequency ablation and cryoablation of epicardial posteroseptal accessory pathways within the coronary venous system. *Circ Arrhythm Electrophysiol* 2014;**7**:113–9.
16. Sun Y, Arruda M, Otomo K, Beckman K, Nakagawa H, Calame J *et al*. Coronary sinus-ventricular accessory connections producing posteroseptal and left posterior accessory pathways: incidence and electrophysiological identification. *Circulation* 2002;**106**:1362–7.
17. Haissaguerre M, Dartigues JF, Warin JF, Le Metayer P, Montserrat P, Salamon R. Electrogram patterns predictive of successful catheter ablation of accessory pathways. Value of unipolar recording mode. *Circulation* 1991;**84**:188–202.
18. Hocini M, Shah AJ, Cochet H, Maury P, Denis A, Haissaguerre M. Noninvasive electrocardiographic facilitates previously failed ablation of right appendage diverticulum associated life-threatening accessory pathway. *J Cardiovasc Electrophysiol* 2013;**24**:583–5.
19. Josephson ME. *Clinical Cardiac Electrophysiology: Techniques and Interpretation*. 2nd ed. Philadelphia: Lea & Febiger; 1993. xi, 83p.
20. Yamada T, Allison JS, McElderry HT, Doppalapudi H, Epstein AE, Plumb VJ *et al*. Successful catheter ablation of premature ventricular contractions originating from the tricuspid annulus using a Halo-type catheter. *Europace* 2008;**10**:1228–9.
21. Yamada T. Twelve-lead electrocardiographic localization of idiopathic premature ventricular contraction origins. *J Cardiovasc Electrophysiol* 2019;**30**:2603–17.